6-23-2015

Resonance of relativistic electrons with electromagnetic ion cyclotron waves

Richard Denton
Dartmouth College

K. Jordanova
Los Alamos National Laboratory

J. Bortnik
University of California, Los Angeles

Resonance of relativistic electrons with electromagnetic ion cyclotron waves

R. E. Denton[1], V. K. Jordanova[2], J. Bortnik[3]

J. Bortnik, Mathematical Sciences Building, Rm 7115, UCLA, Los Angeles, CA, 90095-1565, USA. (jbortnik@gmail.com)

R. E. Denton, 32 Oak Tree Dr., New Smyrna Beach, FL 32169, USA. (richard.e.denton@dartmouth.edu)

V. K. Jordanova, Los Alamos National Lab, MS D466, Los Alamos, NM 87545-0000, USA. (vania@lanl.gov)

[1]Department of Physics and Astronomy, Dartmouth College, Hanover, New Hampshire, USA

[2]Los Alamos National Lab, Los Alamos, New Mexico, USA

[3]Department of Atmospheric and Oceanic Sciences, University of California Los Angeles, Los Angeles, CA, USA

Relativistic electrons have been thought to more easily resonate with electromagnetic ion cyclotron (EMIC) waves if the total density is large. We show that, for a particular EMIC mode, this dependence is weak due to the dependence of the wave frequency and wave vector on the density. A significant increase in relativistic electron minimum resonant energy might occur for the H band EMIC mode only for small density, but no changes in parameters significantly decrease the minimum resonant energy from a nominal value. The minimum resonant energy depends most strongly on the thermal velocity associated with the field line motion of the hot ring current protons that drive the instability. High density due to a plasmasphere or plasmaspheric plume could possibly lead to lower minimum resonance energy by causing the He band EMIC mode to be dominant. We demonstrate these points using parameters from a ring current simulation.

1. Introduction

Relativistic electrons are commonly thought to strongly interact with magnetospheric waves when they are in resonance [*Kennel and Petschek*, 1966; *Shprits et al.*, 2008; *Albert and Bortnik*, 2009]. The resonance condition is

$$\omega - k_{\parallel} v_{\parallel} = -n \frac{\Omega_{\mathrm{ce}}}{\gamma}, \tag{1}$$

where ω is the wave frequency; $k_{\parallel}$ is the component of the wave vector parallel to the background magnetic field; $v_{\parallel}$ is the parallel component of the relativistic electron velocity v; n is the order of the resonance; $\Omega_{\mathrm{ce}} = eB/m_{\mathrm{e}}$ is the nonrelativistic electron cyclotron frequency, where e is the absolute value of the electron charge, B is the background magnetic field, and m_{e} is the electron rest mass; and $\gamma = 1/\sqrt{1-(v/c)^2}$ is the relativistic factor for the electron.

Here we want to consider resonance with electromagnetic ion cyclotron (EMIC) waves [*Cornwall*, 1965; *Kennel and Petschek*, 1966; *Anderson et al.*, 1996; *Meredith et al.*, 2003; *Denton et al.*, 2014; *Li et al.*, 2014]. We want to find the lowest energy relativistic electron that can resonate with the waves. EMIC waves are predominantly transverse, but as the waves propagate away from the magnetic equator, they can become oblique and develop a nonzero parallel electric field. In that case the so called Landau resonance with $n = 0$ might occur, but that interaction would be with low energy electrons with parallel velocity comparable to the Alfvén speed. The lowest energy interaction with relativistic electrons would occur for $n = 1$; for $n = 1$, $v_{\parallel}$ has the same sign as $k_{\parallel}$ in (1), indicating that the resonant electrons move in the same direction as the wave. Henceforth, we will consider only this $n = 1$ resonance.

EMIC waves have real frequency below the proton gyrofrequency. Thus, unless γ in (1) is extremely large, ω in (1) will be utterly negligible compared to $\Omega_{\rm ce}/\gamma$. This means that the relativistic electrons are moving so fast that on the time scale of their motion through the waves, the EMIC waves are essentially static.

The lowest energy particle satisfying (1) would be moving parallel to the background magnetic field $\mathbf{B}$, so that $v_\parallel = v = c\sqrt{1-1/\gamma^2}$. Then, dropping the ω term in (1), the minimum energy particle having $\gamma = \gamma_{\rm min}$ would have

$$\overline{p}_{\rm min} \equiv \gamma_{\rm min}\frac{v_{\rm min}}{c} = \gamma_{\rm min}\sqrt{1-\frac{1}{\gamma_{\rm min}^2}} = \frac{\Omega_{\rm ce}}{ck_\parallel}. \tag{2}$$

The quantity $\overline{p}_{\rm min}$ is the minimum relativistic momentum of the electron $p_{\rm min}$ normalized to $m_{\rm e}c$; $\overline{p}_{\rm min} \approx \gamma_{\rm min}$ for large $\gamma_{\rm min}$, but $\overline{p}_{\rm min} \approx v/c$ as $\gamma_{\rm min}$ approaches unity. The value of $\overline{p}_{\rm min}$ monotonically increases with respect to the total energy of the electron, $\gamma_{\rm min} m_{\rm e} c^2$, and therefore also monotonically increases with respect to the kinetic energy of the electron $E_{\rm K,min} = (\gamma_{\rm min}-1)m_{\rm e}c^2$. So the larger the value of $k_\parallel$ (shorter wavelength), the smaller the value of $\overline{p}_{\rm min}$ corresponding to smaller $E_{\rm K,min}$. Given $\overline{p}_{\rm min}$, $\gamma_{\rm min} = \sqrt{1+\overline{p}_{\rm min}^2}$, and therefore

$$E_{\rm K,min} = \left(\sqrt{1+\overline{p}_{\rm min}^2} - 1\right) m_{\rm e} c^2 \tag{3}$$

[see also *Silin et al.*, 2011].

For a multi-species plasma with singly charged ions of species s, the dispersion relation for electromagnetic ion cyclotron waves is [*Swanson*, 2003; *Denton et al.*, 2014]

$$\overline{k}_\parallel^2 = \overline{\omega}\left(\sum_s \frac{\eta_s}{1-\overline{m}_s\overline{\omega}} - 1\right). \tag{4}$$

Here the overbars indicate normalized quantities, where we have normalized distances to $c/\omega_{\rm pp}$ and inverse time to $\Omega_{\rm cp}$; the proton plasma frequency is $\omega_{\rm pp} \equiv \sqrt{n_{\rm e} e^2/m_{\rm p}\epsilon_0}$; the proton cyclotron frequency is $\Omega_{\rm cp} \equiv eB/m_{\rm p}$; $n_{\rm e}$ is the electron density; $m_{\rm p}$ is the proton mass; ϵ_0 is the vacuum permittivity; the ion species concentration $\eta_s \equiv n_s/n_{\rm e}$; and the normalized ion mass $\overline{m}_s \equiv m_s/m_{\rm p}$. Using the normalized $\overline{k}_\parallel \equiv k_\parallel c/\omega_{\rm pp}$, (2) can be written as

$$\overline{p}_{\rm min} = \frac{\Omega_{\rm ce}}{\omega_{\rm pp}} \frac{1}{\overline{k}_\parallel} = \sqrt{\frac{m_{\rm p}}{m_{\rm e}}} \frac{\Omega_{\rm ce}}{\omega_{\rm pe}} \frac{1}{\overline{k}_\parallel}, \tag{5}$$

where $\omega_{\rm pe} \equiv \sqrt{n_{\rm e} e^2/m_{\rm e}\epsilon_0}$ is the electron plasma frequency.

If one assumes that the EMIC waves have a certain normalized frequency, $\overline{\omega} \equiv \omega/\Omega_{\rm cp}$, independent of the value of $\omega_{\rm pp} \propto \sqrt{n_{\rm e}}$, then (4) shows that $\overline{k}_\parallel$ will also not depend on $\omega_{\rm pp}$. Then (5) shows that $\overline{p}_{\rm min}$ will be proportional to $n_{\rm e}^{-1/2}$. This indicates that larger total density will allow lower energy electrons to resonate with the EMIC waves, and this is one reason that the outer plasmasphere and plasmaspheric plume are considered to be good locations for interaction between EMIC waves and relativistic electrons.

But recently, *Denton et al.* [2014] showed that $\overline{\omega}$ decreases with respect to $n_{\rm e}$ in a way that can be described by a simple formula (their equation (6) and our equation (8) derived in section 2). If $\overline{\omega}$ decreases with respect to $n_{\rm e}$, (4) shows that $\overline{k}_\parallel$ also generally decreases with respect to $n_{\rm e}$ (except very near resonances [*Denton et al.*, 2014]). The $\overline{k}_\parallel$ dependence, decreasing with respect to $n_{\rm e}$, will thus tend to counteract the $\omega_{\rm pe}$ dependence, increasing with respect to $n_{\rm e}$, in (5).

In this paper, we will examine the dependence of $\overline{p}_{\rm min}$ on $n_{\rm e}$ as well as on the ion species concentrations η_s, in order to better understand the conditions under which relativistic

electrons most easily resonate with EMIC waves. We find that for a particular EMIC wave mode, $\overline{p}_{\mathrm{min}}$ depends most strongly on the hot ring current thermal velocity associated with parallel motion, $v_{\mathrm{th}\|\mathrm{h}}$ (defined below). In section 2 we will show our results, and in section 3, we will discuss and summarize these results.

2. Dependence of $\overline{p}_{\mathrm{min}}$ on density and ion composition

Denton et al. [2014] assumed that EMIC waves are driven by a bi-Maxwellian distribution of hot ring current protons such that the wave is in Doppler resonance with Ω_{cp} for the hot protons with a parallel velocity equal to their parallel thermal speed, $v_{\mathrm{th}\|\mathrm{h}} \equiv \sqrt{2k_B T_{\|\mathrm{h}}/m_{\mathrm{p}}}$, moving in the direction opposite to that of the wave ($k_\|$ and $v_\|$ in (1) have opposite sign), so that

$$\omega + k_\| v_{\mathrm{th}\|\mathrm{h}} = \Omega_{\mathrm{cp}}. \tag{6}$$

Here k_B is the Boltzmann constant, and $T_{\|\mathrm{h}}$ is the hot proton temperature associated with motion along the magnetic field. Equation (6) can be written as

$$\overline{k}_\| \sqrt{\beta_{\|\mathrm{h,e}}} = 1 - \overline{\omega}, \tag{7}$$

where $\beta_{\|\mathrm{h,e}} \equiv n_{\mathrm{e}} k_{\mathrm{B}} T_{\|\mathrm{h}}/(B^2/(2\mu_0))$ is the hybrid plasma beta calculated using the parallel temperature of the hot protons with the total electron density n_{e}; it could also be written as $\beta_{\|\mathrm{h}} n_{\mathrm{e}}/n_{\mathrm{h}}$, where $\beta_{\|\mathrm{h}}$ is the plasma beta of the hot ring current protons defined using the parallel temperature.

Combining (7) with (4), Denton et al. found

$$\frac{\overline{\omega}}{(1-\overline{\omega})^2}\left(\sum_s \frac{\eta_s}{1-\overline{m}_s\overline{\omega}} - 1\right) = \frac{1}{\beta_{\|\mathrm{h,e}}}, \tag{8}$$

and they showed that this equation well predicted the most unstable frequencies of EMIC waves using plasma parameters from a ring current simulation of an event during which EMIC waves were observed. For detailed information about this simulation, see the description of *Denton et al.* [2014]; for our purposes here, the parameters shown in Figure 1 for Denton et al.'s "constant cold composition" simulation will be sufficient for a sample case. For an H+/He+/O+ plasma, EMIC waves occur in three bands, the H band, the He band, and the O band, where the frequency of the band approaches the gyrofrequency of the named ion species (for a cold plasma) for large $k_\parallel$. Figure 1d shows $\overline{\omega} \equiv \omega/\Omega_{\rm cp}$ for the H and He band EMIC modes (from Figure 10a of *Denton et al.* [2014]). The solid curves in Figure 1d show the prediction of the simple model in (8), while the asterisks were found from kinetic theory, and the "o" symbols were found from a hybrid code simulation. The rough agreement of these different symbols validates the assumption of (6).

We can rearrange (5) to get

$$\overline{p}_{\rm min} = \left(\frac{m_{\rm p}}{m_{\rm e}}\frac{v_{\rm th\parallel h}}{c}\right)\left(\frac{1}{\overline{k}_\parallel\sqrt{\beta_{\rm \parallel h,e}}}\right) \tag{9}$$

$$= \left(\frac{m_{\rm p}}{m_{\rm e}}\frac{v_{\rm th\parallel h}}{c}\right)\left(\frac{1}{1-\overline{\omega}}\right), \tag{10}$$

where we used (7) to find (10). In (9) or (10), the terms in the left parentheses depend only on $v_{\rm th\parallel h}$, or equivalently, on $T_{\rm \parallel h}$. Only the terms in the second parentheses depend on $n_{\rm e}$. Also, $\beta_{\rm \parallel h,e} \propto n_{\rm e}$. Therefore, we can see the dependence of $\overline{p}_{\rm min}$ on $n_{\rm e}$ by plotting $\left(\overline{k}_\parallel\sqrt{\beta_{\rm \parallel h,e}}\right)^{-1}$, or equivalently, $(1-\overline{\omega})^{-1}$, versus $\beta_{\rm \parallel h,e}$. We will discuss the dependence on $v_{\rm th\parallel h}$ in section 3.

The dependence of $\overline{p}_{\rm min}$ on $\overline{\omega}$ in (10) is the opposite of many people's expectation. Larger $\overline{\omega}$ leads to larger $\overline{p}_{\rm min}$. We emphasize that if $\overline{\omega}$ could be varied independently of

the plasma parameters, then larger $\overline{\omega}$ would correspond to larger $\overline{k}_\parallel$ (from equation (4)). But we are assuming that the ring current protons must be in resonance with the wave. Then (6) shows that higher frequency corresponds to smaller wave number, given that $v_{\mathrm{th}\|\mathrm{h}}$ is held constant.

The term $\left(\overline{k}_\parallel\sqrt{\beta_{\|\mathrm{h,e}}}\right)^{-1} = (1-\overline{\omega})^{-1}$ can only be large if $\overline{\omega}$ approaches unity. This means that the only mode for which $\left(\overline{k}_\parallel\sqrt{\beta_{\|\mathrm{h,e}}}\right)^{-1}$ could possibly deviate greatly from unity is the H band EMIC mode. Note that for the He band EMIC mode, the variation of $(1-\overline{\omega})^{-1}$ could only range between 16/15 for $\overline{\omega} = 1/16$ (He band cutoff frequency at the O+ gyrofrequency) to 4/3 for $\overline{\omega} = 1/4$ at the He+ gyrofrequency resonance, a total range of a factor of 1.25.

We now choose these nominal parameters, $\beta_{\|\mathrm{h,e}} = 10$, $\eta_{\mathrm{He+}} = 0.1$, and $\eta_{\mathrm{O+}} = 0.01$ for an H+/He+/O+ plasma. Keeping one or two of these parameters constant and varying the other parameters, we will examine the resulting variation in $\overline{p}_{\min}$. In each case, $\eta_{\mathrm{H+}} = 1 - \eta_{\mathrm{He+}} - \eta_{\mathrm{O+}}$; $\overline{\omega}$ is found from (8) using a numerical root solver; and $\overline{k}_\parallel$ is found from (4).

2.1. Density dependence

Keeping $\eta_{\mathrm{He+}} = 0.1$ and $\eta_{\mathrm{O+}} = 0.01$, we plot $\overline{\omega}$, $\overline{k}_\parallel$, and $(1-\overline{\omega})^{-1} = \left(\overline{k}_\parallel\sqrt{\beta_{\|\mathrm{h,e}}}\right)^{-1}$ versus $\beta_{\|\mathrm{h,e}}$ in Figure 2 for the H band EMIC mode (black solid curve), the He band EMIC mode (blue curve), and the O band EMIC mode (red curve). Note that the cutoff frequencies occur at the right side of the plot, where $\overline{k}_\parallel$ is small, and the resonance frequencies are approached at the left side of the plot.

As noted previously, $\overline{\omega}$ decreases with respect to $\beta_{\|\mathrm{h,e}} \propto n_{\mathrm{e}}$ for each mode (Figure 2a). Consequently, $\overline{k}_{\|}$ decreases with respect to $\beta_{\|\mathrm{h,e}}$ for each mode (Figure 2b). The value of $\overline{k}_{\|}$ is nearly proportional to $\beta_{\|\mathrm{h,e}}^{-0.5}$ (slope of diagonal dotted black line in Figure 2b). As suggested by (7), large departures from this relationship only occur where $\overline{\omega}$ approaches unity.

Therefore, as noted above, the largest variation in $(1-\overline{\omega})^{-1} = \left(\overline{k}_{\|}\sqrt{\beta_{\|\mathrm{h,e}}}\right)^{-1}$ is for the H band EMIC mode (black solid curve in Figure 2c), and particularly for $\beta_{\|\mathrm{h,e}} < 1$. In that case, low values of $\beta_{\|\mathrm{h,e}}$ lead to large values of $\overline{p}_{\mathrm{min}}$, indicating that it is more difficult for low energy relativistic electrons to resonate with the waves. But the EMIC mode may not be unstable for such small values of $\beta_{\|\mathrm{h,e}}$ [*Blum et al.*, 2009].

Note also that $(1-\overline{\omega})^{-1}$ is lower for He band EMIC than for H band EMIC, indicating that it is easier for low energy relativistic electrons to resonate with the He band waves. This is because, given the same value of $v_{\mathrm{th}\|\mathrm{h}}$, a larger value of $k_{\|}$ is required to Doppler shift the wave frequency up to Ω_{cp} from the lower frequency (equation (6)). (It would be even easier for low energy relativistic electrons to resonate with O band waves, but O band waves are not as common as waves in the H and He bands.)

2.2. Composition dependence

Figure 3 shows the same quantities that were plotted in Figure 2, but plotted versus $\eta_{\mathrm{He+}}$ holding $\eta_{\mathrm{O+}} = 0.01$ constant in column a, and versus $\eta_{\mathrm{O+}}$ holding $\eta_{\mathrm{He+}} = 0.1$ constant in column b. In both cases, $\beta_{\|\mathrm{h,e}} = 10$ is constant. With $\beta_{\|\mathrm{h,e}}$ constant, (9) shows that the concentration of ions species η_s affects the value of $\overline{p}_{\mathrm{min}}$ through the term $(1-\overline{\omega})^{-1}$.

The presence of heavy ions (heavier than the species name for the EMIC wave band) leads to an increase in $\overline{\omega}$ [*Denton et al.*, 2014]. From Figure 3Ca and Cb, we see that $(1-\overline{\omega})^{-1}$ is close to unity except for the H band EMIC mode at large values of heavy ion concentration. In that case, large concentration of He+ or O+ leads to large values of $\overline{p}_{\rm min}$, indicating that it is more difficult for low energy relativistic electrons to resonate with the waves.

3. Discussion

We have shown that the minimum resonant energy, characterized by $\overline{p}_{\rm min} \equiv \gamma_{\rm min}\sqrt{1-\frac{1}{\gamma_{\rm min}^2}} \propto \left(\overline{k}_\| \sqrt{\beta_{\|{\rm h,e}}}\right)^{-1} = (1-\overline{\omega})^{-1}$ (equations (2), (9), and (10)), is only weakly dependent on $\beta_{\|{\rm h,e}} \propto n_{\rm e}$ (Figure 2) and the heavy ion concentrations $\eta_{\rm He+}$ (Figure 3Ca) and $\eta_{\rm O+}$ (Figure 3Cb) for a particular wave mode. The only significant dependence on these quantities is for the H band EMIC mode. For that mode, the strongest dependence on $\beta_{\|{\rm h,e}}$ is for very low values, but at very low values of $\beta_{\|{\rm h,e}}$, EMIC waves may not be unstable [*Blum et al.*, 2009]. The heavy ions only have a significant effect at large $\eta_{\rm He+}$ or $\eta_{\rm O+}$. For $\sqrt{\beta_{\|{\rm h,e}}}$ or $\eta_{\rm s}$, strong dependence only occurs as $\overline{\omega}$ approaches unity. But in order for EMIC waves to grow with large $\overline{\omega}$, the temperature anisotropy of the hot ring current protons, $A_{\rm h} \equiv T_{\perp{\rm h}}/T_{\|{\rm h}} - 1$, must be large. From Equation 2.23 of *Kennel and Petschek* [1966], $A_{\rm h} \geq \overline{\omega}/(1-\overline{\omega})$. So, for instance, $\overline{\omega} = 0.8$ would require $A_{\rm h} = 4$ or $T_{\perp{\rm h}}/T_{\|{\rm h}} = 5$, which is rare.

Large $\overline{\omega}$ leads to large $\overline{p}_{\rm min}$ making resonance with relativistic electrons more difficult. Variations in $\beta_{\|{\rm h,e}}$, $\eta_{\rm He+}$, and $\eta_{\rm O+}$ do not cause large decreases in $\left(\overline{k}_\| \sqrt{\beta_{\|{\rm h,e}}}\right)^{-1} = (1-\overline{\omega})^{-1}$. The maximum value of $\overline{k}_\| \sqrt{\beta_{\|{\rm h,e}}}$ occurs with the lowest possible value of $\overline{\omega}$, meaning that

the Doppler term must shift the wave frequency up by the maximum amount (equation (6)). But the value of $\overline{\omega}$ will be at least zero, leading to $(1-\overline{\omega})^{-1} = 1$. For the He band EMIC mode, often thought to be most important for relativistic electron pitch angle scattering, $(1-\overline{\omega})^{-1}$ is always close to unity since $\overline{\omega}$ varies only between 1/16 (O+ gyrofrequency) and 1/4 (He+ gyrofrequency).

Based on these facts, the largest dependence of $\overline{p}_{\rm min}$ for a particular mode is not on $\beta_{\|{\rm h,e}} \propto n_{\rm e}$, $\eta_{\rm He+}$, or $\eta_{\rm O+}$, but on $v_{\rm th\|h} \propto \sqrt{T_{\|\rm h}}$ (equation (9) or (10)), since $\overline{p}_{\rm min} \propto v_{\rm th\|h}$. That is, it is the parallel temperature of the hot ring current protons driving the EMIC waves that has the greatest impact on the minimum resonant energy. If low energy ring current protons drive the EMIC instability, it will be easier for low energy relativistic electrons to resonate with the waves. A rough approximation to (9), $\gamma = (m_{\rm p}/m_{\rm e})(v_{\rm th\|h}/c)$, follows directly from approximating the ion and electron resonance conditions as $k_\| v_{\rm th\|h} = \Omega_{\rm cp}$ and $k_\| c = \Omega_{\rm ce}/\gamma$, respectively; that is, $\overline{\omega}$ in (10) is taken to be zero.

Now consider again the parameters from the ring current simulation described by *Denton et al.* [2014] and plotted in Figure 1. Figure 1e shows $\overline{p}_{\rm min}$ for the H band mode (black curve) and He band mode (blue curve) calculated using (10) with the hot H+ parallel temperature $T_{\|\rm h}$ from Figure 1a and the normalized wave frequency $\overline{\omega}$ in Figure 1d. The lowest value of $\overline{p}_{\rm min}$ is for the He band EMIC mode, which is also the largest mode growing in the the hybrid code simulation [*Denton et al.*, 2014]. Note from the densities plotted in Figure 1b that the two gray vertical lines roughly delineate the plasmapause, with the plasmasphere to the left of the leftmost gray vertical line, and the plasmatrough to the

right of the rightmost gray vertical line. Despite the fact that the total density is much greater in the plasmasphere, $\overline{p}_{\rm min}$ is smallest in the plasmatrough (region to the right of the rightmost gray vertical line in Figure 1b). This is evidently because of the decrease in $T_{\|{\rm h}}$ shown in Figure 1a.

Figure 1f shows the minimum resonant relativistic electron kinetic energy $E_{\rm K,min}$ calculated using $\overline{p}_{\rm min}$ in (3) for the H band EMIC mode (black solid curve) and He band EMIC mode (blue solid curve). Again, the minimum resonant energy is lower for the He band mode and decreases at large L. To emphasize the functional dependence due to $T_{\|{\rm h}}$ and $\overline{\omega}$, the dotted blue curve is plotted using variation in $T_{\|{\rm h}}$, but holding $\overline{\omega}$ constant $= 0.201$, while the large dashed blue curve is plotted using variation in $\overline{\omega}$, but holding $T_{\|{\rm h}}$ constant $= 7.08$ keV. While the $\overline{\omega}$ dependence does lead to a small decrease in $E_{\rm K,min}$ at low L (large dashed blue curve), the variation in $E_{\rm K,min}$ due to variation in $T_{\|{\rm h}}$ is much larger (dotted blue curve).

Based on these results, if the plasmasphere or plasma plume is a preferred region for resonance of relativistic electrons with EMIC waves, as suggested by *Borovsky et al.* [2014], it's probably not because the cold density makes resonance easier, at least for a particular mode. As mentioned in the Introduction, if the normalized frequency of the waves, $\overline{\omega}$, were independent of $n_{\rm e}$, then the minimum resonant energy would be significantly lower at high $n_{\rm e}$. But *Denton et al.* [2014] showed that $\overline{\omega}$ decreases with respect to $n_{\rm e}$; and we have shown that this causes the minimum resonant energy to vary only very weakly with respect to $n_{\rm e}$.

Values of $E_{\mathrm{K,min}}$ based on the finite temperature kinetic dispersion code Waves in Homogeneous Anisotropic Multicomponent Plasmas (WHAMP) [*Ronnmark*, 1982] are shown in Figure 1f for the He mode at $L = 5.5$ and 6 (blue asterisks) and for the H mode at $L = 6.5$ (black asterisk) at the wave number for which the growth rate normalized to Ω_{cp}, $\overline{\gamma}$, has its maximum value, $\overline{\gamma}_{\mathrm{max}}$. These results are generally in agreement with the simple model (solid curves in Figure 1f).

Two other recent papers have examined the relativistic electron resonance condition using kinetic theory [*Silin et al.*, 2011; *Chen et al.*, 2011]. Both of these claim that high density leads to a lower minimum resonant energy. Chen et al. evaluate the minimum resonant energy for all wave frequencies for which $\overline{\gamma}$ is greater than 0.01. The assumption is that a range of frequencies can be excited, and that the entire spectrum needs to be considered. While it's certainly true that the full spectrum of waves can resonate with relativistic electrons [*Ukhorskiy et al.*, 2010], it's not totally clear how to calculate the nonlinear spectrum of waves based on linear theory. At the least, this will depend sensitively on the initial noise level from which the waves grow.

Also, when parameters are varied independently, unrealistic combinations may result. For instance, the majority of cases described by *Silin et al.* [2011] have unrealistically high plasma beta. In their sweep of parameter space, *Chen et al.* [2011] do not mention the range of any parameter indicating instability [like that of *Blum et al.*, 2009], but given the range of parameter space explored, some of the cases considered may have been unrealistically unstable.

Larger growth rate leads to a greater range of frequencies that are unstable, and the higher frequencies, corresponding to larger wave number (not necessarily satisfying (6)), will have lower minimum resonant energy. *Chen et al.* [2011] find a correlation between increasing hot proton density n_{h}, hot proton temperature anisotropy, $A_{\mathrm{h}} \equiv T_{\perp \mathrm{h}}/T_{\|\mathrm{h}} - 1$, and total density with lower minimum resonant energy. We find using WHAMP (not shown) that there is only a small change in $E_{\mathrm{K,min}}$ at $\overline{\gamma} = \overline{\gamma}_{\mathrm{max}}$ when the cold ion densities are increased, and that there is almost no change in $E_{\mathrm{K,min}}$ at $\overline{\gamma} = \overline{\gamma}_{\mathrm{max}}$ when n_{h} or A_{h} are increased. These results are consistent with the simple theory we have presented. But an increase in total density, n_{h}, or A_{h}, does lead to a more unstable plasma, yielding lower $E_{\mathrm{K,min}}$ within the range of unstable frequencies.

A more realistic way to vary the parameters might be to keep the instability condition [*Blum et al.*, 2009] roughly constant. The ring current parameters tend to be regulated close to a marginal stability condition [*Gary et al.*, 1994; *Denton et al.*, 1994; *Blum et al.*, 2009]. For this reason, we have concentrated on the most unstable mode. We expect this mode to be the most intense, and hence to do the majority of the scattering [*Bortnik et al.*, 2010].

Relativistic electron precipitation events observed by balloons tend to be clustered around dusk local time. The relation $\overline{p}_{\mathrm{min}} \propto v_{\mathrm{th}\|\mathrm{h}}$ would suggest that low energy electrons might more easily resonate with EMIC waves at dawn or pre-dawn local time, where the ring current protons are typically of lower energy [*Anderson et al.*, 1996; *Lee and Angelopoulos*, 2014]. But there are other factors that come into play, such as higher con-

centration of O+ at dawn [*Denton et al.*, 2012; *Lee and Angelopoulos*, 2014] and better conditions for growth of large amplitude waves at dusk [*Denton et al.*, 2014].

Theoretically, enhanced resonance of relativistic electrons with EMIC waves in the plasmasphere or plume could result from larger growth of EMIC waves when the bulk density is large [*Jordanova et al.*, 2008; *Denton et al.*, 2014]. There is some support for a correlation between plasma density and EMIC waves, though the result is not unequivocal [*Fraser et al.*, 2005; *Halford et al.*, 2015; *Usanova et al.*, 2013]. We are not aware of a study showing that $T_{\|\mathrm{h}}$ is normally lower in the plasmasphere or plume, and such a correlation is not supported by the ring current simulation results plotted in Figure 1a, for which $T_{\|\mathrm{h}}$ is greater in the plasmasphere.

High density at dusk is particularly conducive to producing He mode EMIC waves [*Denton et al.*, 2014; *Lee and Angelopoulos*, 2014]. Figure 1f shows that $E_{\mathrm{K,min}}$ is lower for He band EMIC than for H band EMIC. So if high density causes the He mode to be dominant, that would lead to lower minimum resonance energies. In fact, the He band EMIC mode is stable for the plasma parameters in Figure 1 outside the plasmapause at $L = 6.5$. So considering the available wave modes, the minimum resonance energy is lower at $L = 5.5$ than at $L = 6.5$ (comparing the blue asterisk at $L = 5.5$ in Figure 1f to the black asterisk at $L = 6.5$).

It is also possible that non-resonant interactions could significantly affect the radiation belt electrons. More work needs to be done to examine the pitch angle scattering of relativistic electrons in realistic EMIC wave fields.

Acknowledgments. We thank Mary Hudson and Jay Albert for useful conversations. Work at Dartmouth was supported by NASA grants NNX10AQ60G, NNX13AD65G, and NNX08AM58G. Work at Los Alamos was conducted under the auspices of the U. S. Department of Energy with partial support from NASA grant NNH13AW83I and NSF grant IAA1203460. JB would like to acknowledge support from NSF/DOE basic plasma physics grant DE-SC0010578. Numerical data shown in this paper are available from the lead author upon request.

References

Albert, J. M., and J. Bortnik (2009), Nonlinear interaction of radiation belt electrons with electromagnetic ion cyclotron waves, *Geophys. Res. Lett.*, p. L12110 (5 pp.), doi: 10.1029/2009gl03 8904.

Anderson, B. J., R. E. Denton, G. Ho, D. C. Hamilton, S. A. Fuselier, and R. J. Strangeway (1996), Observational test of local proton cyclotron instability in the earth's magnetosphere, *J. Geophys. Res.*, *101*(A10).

Blum, L. W., E. A. MacDonald, S. P. Gary, M. F. Thomsen, and H. E. Spence (2009), Ion observations from geosynchronous orbit as a proxy for ion cyclotron wave growth during storm times, *J. Geophys. Res.*, *114*, doi:10.1029/2009ja014396.

Borovsky, J. E., R. H. W. Friedel, and M. H. Denton (2014), Statistically measuring the amount of pitch angle scattering that energetic electrons undergo as they drift across the plasmaspheric drainage plume at geosynchronous orbit, *J. Geophys. Res.*, *119*(3), 1814–1826, doi:10.1002/2013ja019310.

Bortnik, J., R. M. Thorne, and N. Omidi (2010), Nonlinear evolution of EMIC waves in a uniform magnetic field: 2. Test-particle scattering, *J. Geophys. Res.*, *115*, a12242, doi:10.1029/2010ja015603.

Chen, L., R. M. Thorne, and J. Bortnik (2011), The controlling effect of ion temperature on EMIC wave excitation and scattering, *Geophys. Res. Lett.*, *38*, l16109, doi: 10.1029/2011gl048653.

Cornwall, J. M. (1965), Cyclotron instabilities and electromagnetic emission in ultra low frequency and very low frequency ranges, *Journal of Geophysical Research*, *70*(1), 61, doi:10.1029/JZ070i001p00061.

Denton, R. E., B. J. Anderson, S. P. Gary, and S. A. Fuselier (1994), Bounded anisotropy fluid model for ion temperatures, *J. Geophys. Res.*, *99*(A6).

Denton, R. E., K. Takahashi, and M. F. Thomsen (2012), O+ concentration at geosynchronous orbit, Abstract SA31C-01, in *2012 Fall Meeting, AGU, San Francisco, Calif., 3-7 Dec.*

Denton, R. E., V. K. Jordanova, and B. J. Fraser (2014), Effect of spatial density variation and O+ concentration on the growth and evolution of electromagnetic ion cyclotron waves, *J. Geophys. Res.*, *119*(10), 8372–8395, doi:10.1002/2014ja020384.

Fraser, B. J., H. J. Singer, M. L. Adrian, and D. L. Gallagher (2005), The relationship between plasma density structure and EMIC waves at geosynchronous orbit, in *Inner Magnetosphere Interactions: New Perspectives from Imaging, Geophys. Monog. Ser., vol. 159*, edited by J. L. Burch, M. Schulz, and H. Spence, pp. 55 – 70, AGU, Washington, D. C.

Gary, S. P., B. J. Anderson, R. E. Denton, S. A. Fuselier, and M. E. McKean (1994), A limited closure relation for anisotropic plasmas from the Earths magnetosheath, *Phys. Plasmas*, *1*(5).

Halford, A. J., B. J. Fraser, and S. K. Morley (2015), EMIC waves and plasmaspheric and plume density: CRRES results, *J. Geophys. Res.*, *120*, 19741992, doi: 10.1002/2014JA020338.

Jordanova, V. K., J. Albert, and Y. Miyoshi (2008), Relativistic electron precipitation by EMIC waves from self-consistent global simulations, *J. Geophys. Res.*, *113*, a00a10, doi:10.1029/2008ja013239.

Kennel, C. F., and H. E. Petschek (1966), Limit on stably trapped particle fluxes, *Journal of Geophysical Research*, *71*(1), 1.

Lee, J. H., and V. Angelopoulos (2014), Observations and modeling of EMIC wave properties in the presence of multiple ion species as function of magnetic local time, *J. Geophys. Res.*, *119*(11), 8942–8970, doi:10.1002/2014ja020469.

Li, Z., et al. (2014), Investigation of EMIC wave scattering as the cause for the BARREL 17 January 2013 relativistic electron precipitation event: A quantitative comparison of simulation with observations, *Geophys. Res. Lett.*, *41*(24), 8722–8729, doi: 10.1002/2014gl062273.

Meredith, N. P., R. M. Thorne, R. B. Horne, D. Summers, B. J. Fraser, and R. R. Anderson (2003), Statistical analysis of relativistic electron energies for cyclotron resonance with EMIC waves observed on CRRES, *J. Geophys. Res.*, *108*(A6), 1250, doi: 10.1029/2002ja009700.

Ronnmark, K. (1982), Waves in homogeneous, anisotropic, multicomponent plasmas, *Tech. Rep. Kiruna Geophys. Inst. Rep. 179, 56 pp.*, Swedish Institute of Space Physics, Univ. of Umea, Sweden.

Shprits, Y. Y., S. R. Elkington, N. P. Meredith, and D. A. Subbotin (2008), Review of modeling of losses and sources of relativistic electrons in the outer radiation belt i: Radial transport, *J. Atmos. Sol.-Terr. Phys.*, *70*(14), 1679–1693, doi:10.1016/j.jastp.2008.06.008.

Silin, I., I. R. Mann, R. D. Sydora, D. Summers, and R. L. Mace (2011), Warm plasma effects on electromagnetic ion cyclotron wave MeV electron interactions in the magnetosphere, *J. Geophys. Res.*, *116*, a05215, doi:10.1029/2010ja016398.

Swanson, D. G. (2003), *Plasma Waves*, 2nd ed., Institute of Physics Publishing, Bristol and Philadelphia.

Ukhorskiy, A. Y., Y. Y. Shprits, B. J. Anderson, K. Takahashi, and R. M. Thorne (2010), Rapid scattering of radiation belt electrons by storm-time emic waves, *Geophys. Res. Lett.*, *37*, l09101, doi:10.1029/2010gl042906.

Usanova, M. E., F. Darrouzet, I. R. Mann, and J. Bortnik (2013), Statistical analysis of EMIC waves in plasmaspheric plumes from Cluster observations, *J. Geophys. Res.*, *118*(8), 4946–4951, doi:10.1002/jgra.50464.

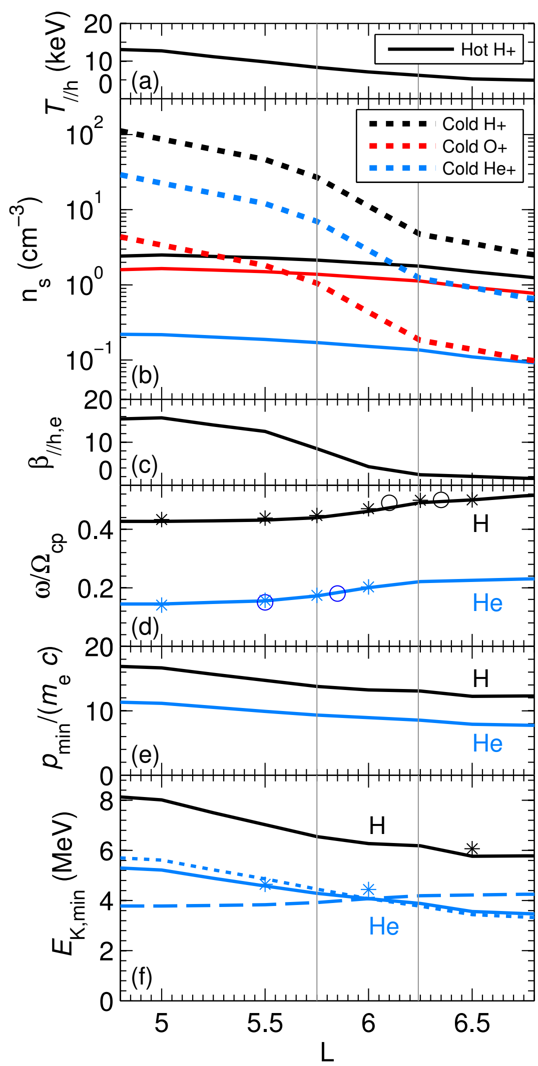

Figure 1. Using parameters from the ring current simulation described by *Denton et al.* [2014], (a) $T_{\parallel h}$ for hot H+, (b) density n_s for different particle species s (solid curves for hot populations and dotted curves for cold populations) in cm^{-3}, (c) hybrid plasma beta $\beta_{\parallel \mathrm{h,e}}$, (d) $\overline{\omega} \equiv \omega/\Omega_{\mathrm{cp}}$ for H band EMIC (black solid curve) and He band EMIC (blue solid curve), and (e) $\overline{p}_{min} \equiv p_{\mathrm{min}}/(m_{\mathrm{e}}c)$ and (f) minimum resonant kinetic energy $E_{\mathrm{K,min}}$ (solid curves) for interaction of relativistic electrons with the wave frequencies that were plotted in panel c; these are all plotted versus L. The other symbols in the plot are described in the text.

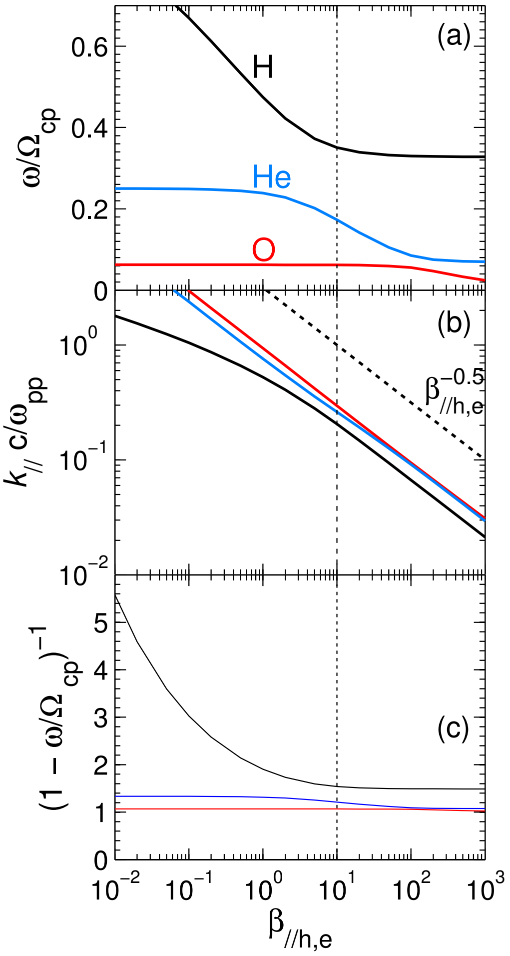

Figure 2. Holding $\eta_{\mathrm{He+}} = 0.1$ and $\eta_{\mathrm{O+}} = 0.01$ constant, (a) $\overline{\omega}$, (b) $\overline{k}_\parallel$, and (c) $(1-\overline{\omega})^{-1} = \left(\overline{k}_\parallel \sqrt{\beta_{\parallel \mathrm{h,e}}}\right)^{-1}$ versus $\beta_{\parallel \mathrm{h,e}}$. Black, blue, and red color correspond respectively to the H, He, and O band EMIC modes. In (b), the diagonal dotted black curve is proportional to $\beta_{\parallel \mathrm{h,e}}^{-0.5}$. The vertical dotted black line is at the nominal value of $\beta_{\parallel \mathrm{h,e}} = 10$ relevant for other plots.

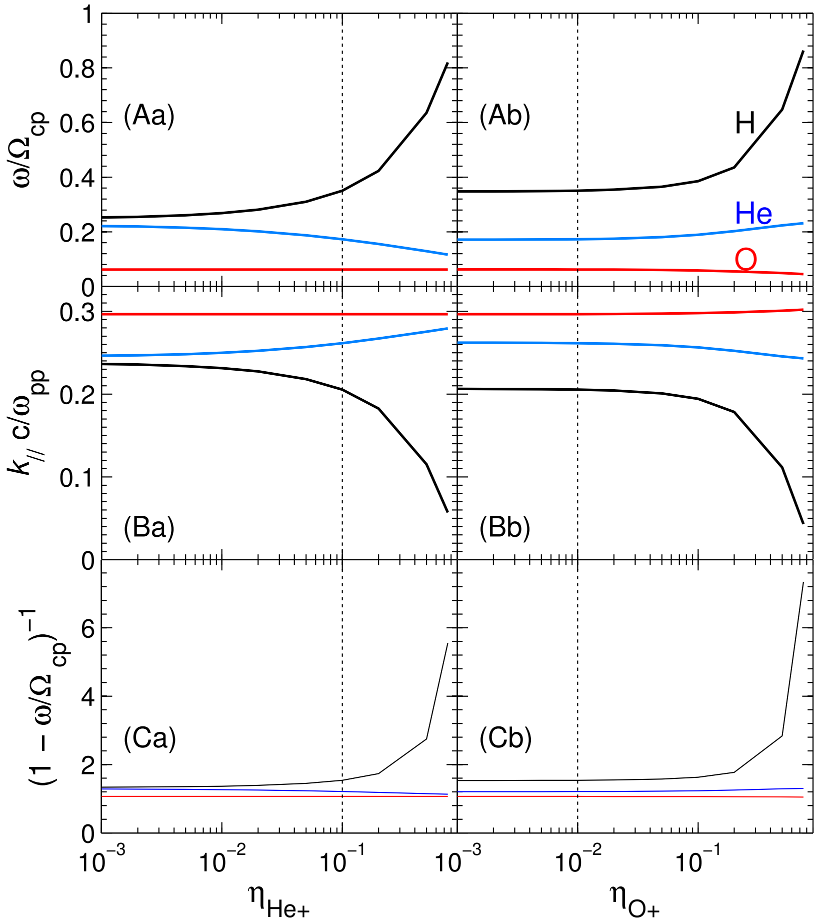

Figure 3. Same quantities as were plotted in Figure 2, but plotted versus $\eta_{\mathrm{He+}}$ holding $\eta_{\mathrm{O+}} = 0.01$ constant in column a, and versus $\eta_{\mathrm{O+}}$ holding $\eta_{\mathrm{He+}} = 0.1$ constant in column b. In both cases, $\beta_{\|\mathrm{h,e}} = 10$ is constant. The vertical dotted black lines are plotted at the nominal values used in other plots, $\eta_{\mathrm{He+}} = 0.1$ in column a, and at $\eta_{\mathrm{O+}} = 0.01$ in column b.